Canonical Realization of Chua's Circuit Family

LEON O. CHUA, FELLOW, IEEE, AND GUI-NIAN LIN

Abstract—**In this paper we present a new canonical piecewise-linear circuit capable of realizing *every* member of the Chua's circuit family [6]. It contains only six two-terminal elements: five of them are linear resistors, capacitors, and inductors, and only one element is a three-segment piecewise-linear resistor. It is canonical in the sense that (1) it can exhibit *all* possible phenomena associated with any three-region symmetric piecewise-linear continuous vector fields, including those defined in [1] and in [2], and more; and (2) it contains the *minimum* number of circuit elements needed for such a circuit.**

Using this circuit, we proved a theorem that specifies the constraint on the types of eigenvalue patterns associated with a piecewise-linear continuous vector field having three equilibrium points. This theorem has an explicit physical meaning and unifies the corresponding theorem in [1] and [2]. We also present some computer simulation results of this circuit, including some new attractors that have not been observed before.

I. Introduction

Among general piecewise-linear systems, the class of three-region symmetric (with respect to the origin) piecewise-linear continuous vector fields (henceforth denoted by $\boldsymbol{L}$) is of particular interest and importance [1]–[10]. It is proved in [1] and [2] that any two vector fields ξ and ξ' in $\boldsymbol{L}$ are *linearly conjugate* if and only if their corresponding eigenvalues in each region are identical, and are *linearly equivalent* if and only if their corresponding normalized eigenvalues in each region are identical. Here, linear conjugacy implies the respective dynamic behaviors are identical, whereas linear equivalence implies *qualitatively* similar dynamic behaviors.

Therefore, if we can build a piecewise-linear circuit whose natural frequencies are equal to an arbitrarily prescribed set of eigenvalues, we can derive all possible phenomena in $\boldsymbol{L}$ by analyzing this one circuit alone. Such an attempt for the most general class of Chua's circuit, called the Chua's circuit family, has been mentioned in [6], but no such circuit has been reported to date.

Although Chua's circuit displays rather rich nonlinear dynamics [8], many phenomena other than those observed from this circuit have been discovered from *other* piecewise-linear circuits belonging to the Chua's circuit family [9], [10]. However, we will prove that not one of these circuits is general enough to satisfy our above-cited objective.

In this paper, we will present a new piecewise-linear circuit. It contains the minimum number of circuit elements needed to generate all possible phenomena in any three-dimensional, three-region continuous and symmetric piecewise-linear vector fields. In Section II, we demonstrate why no existing circuits can fulfill our purpose. In Section III, we give the structure of the canonical piecewise-linear circuit and the explicit formulas for calculating its element parameters from an arbitrarily given set of eigenvalues. In Section IV, based on this circuit, we prove a theorem on the class of realizable eigenvalues, thereby unifying the corresponding theorems in [1] and [2]. In Section V, we present some simulation results, including a few attractors that have not been reported before. For certain eigenvalues where the canonical circuit in Section III requires *negative* dynamic elements, and/or too many *negative* resistors, other equivalent but more practical piecewise-linear circuit realizations are presented in Section VI.

II. Eigenvalue Constraints for Existing Circuits

Consider the class of three-dimensional three-region and symmetric (with respect to the origin) piecewise-linear continuous vector fields. The eigenvalues in the inner region D_0 are denoted by μ_1, μ_2, and μ_3. The eigenvalues in the two outer regions D_{+1} and D_{-1} are equal, since the vector field is symmetric with respect to the origin. We denote them by ν_1, ν_2, and ν_3. Some of the μ's and the ν's may be complex conjugate numbers. In order to avoid complex numbers, let us define

$$p_1 = \mu_1 + \mu_2 + \mu_3; \qquad p_2 = \mu_1\mu_2 + \mu_2\mu_3 + \mu_3\mu_1;$$
$$p_3 = \mu_1\mu_2\mu_3 \tag{1}$$
$$q_1 = \nu_1 + \nu_2 + \nu_3; \qquad q_2 = \nu_1\nu_2 + \nu_2\nu_3 + \nu_3\nu_1;$$
$$q_3 = \nu_1\nu_2\nu_3. \tag{2}$$

Let us analyze the type of eigenvalue patterns that can be produced by Chua's circuit, as shown in Fig. 1(a). The v–i relationship of the nonlinear resistor G_N is shown in

Manuscript received July 12, 1989; revised February 20, 1990. This work was supported in part by the Office of Naval Research under Contract N00014-89-J1402 and by the National Science Foundation under Grant MIP 8912639. This paper was recommended by Associate Editor J. Vandewalle.

L. O. Chua is with the University of California, Berkeley, Berkeley, CA 94720.

G.-N. Lin is with the Department of Electrical Engineering and Computer Sciences, University of California, Berkeley, CA 94720, on leave from the Shanghai Railroad Institute, China.

IEEE Log Number 9035943.

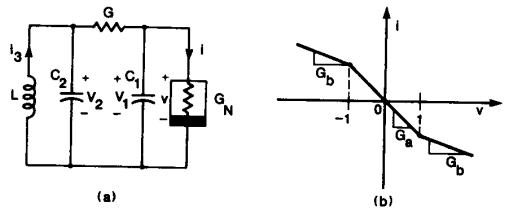

Fig. 1. (a) Chua's circuit. (b) The $v-i$ characteristic of the nonlinear resistor G_N.

Fig. 1(b). The state equations of this circuit are

$$\frac{dv_1}{dt} = \frac{1}{C_1}\left[G(v_2 - v_1) - \left(G_b v_1 + \frac{1}{2}(G_a - G_b)(|v_1 + 1| - |v_1 - 1|)\right)\right]$$

$$\frac{dv_2}{dt} = \frac{1}{C_2}[G(v_1 - v_2) + i_3] \tag{3}$$

$$\frac{di_3}{dt} = -\frac{v_2}{L}$$

where we have chosen $v_1 = \pm 1$ as the break points for simplicity.

In the D_0 region, the state equations are linear

$$\begin{bmatrix} \frac{dv_1}{dt} \\ \frac{dv_2}{dt} \\ \frac{di_3}{dt} \end{bmatrix} = \begin{bmatrix} \frac{-(G+G_a)}{C_1} & \frac{G}{C_1} & 0 \\ \frac{G}{C_2} & \frac{-G}{C_2} & \frac{1}{C_2} \\ 0 & \frac{-1}{L} & 0 \end{bmatrix} \begin{bmatrix} v_1 \\ v_2 \\ i_3 \end{bmatrix} = \boldsymbol{M}_0 \begin{bmatrix} v_1 \\ v_2 \\ v_3 \end{bmatrix} \tag{4}$$

where $\boldsymbol{M}_0$ is a constant matrix.

The characteristic equation of $\boldsymbol{M}_0$ is

$$|s1 - \boldsymbol{M}_0| = s^3 + s^2\left(\frac{G}{C_2} + \frac{G}{C_1} + \frac{G_a}{C_1}\right) + s\left(\frac{GG_a}{C_1C_2} + \frac{1}{LC_2}\right) + \frac{G + G_a}{LC_1C_2} = 0. \tag{5}$$

On the other hand, since μ_1, μ_2, and μ_3 are the eigenvalues we want this system to possess, we have

$$(s - \mu_1)(s - \mu_2)(s - \mu_3) = s^3 - p_1 s^2 + p_2 s - p_3 = 0. \tag{6}$$

Comparing (5) with (6), we obtain

$$\frac{G}{C_2} + \frac{G}{C_1} + \frac{G_a}{C_1} = -p_1 \tag{7}$$

$$\frac{GG_a}{C_1C_2} + \frac{1}{LC_2} = p_2 \tag{8}$$

$$\frac{G + G_a}{LC_1C_2} = -p_3. \tag{9}$$

Similarly, in the $D_{\pm 1}$ regions we have

$$\frac{G}{C_2} + \frac{G}{C_1} + \frac{G_b}{C_1} = -q_1 \tag{10}$$

$$\frac{GG_b}{C_1C_2} + \frac{1}{LC_2} = q_2 \tag{11}$$

$$\frac{G + G_b}{LC_1C_2} = -q_3. \tag{12}$$

Subtracting (10) from (7), (11) from (8), and (12) from (9), we obtain

$$\frac{G_a - G_b}{C_1} = -p_1 + q_1 \tag{13}$$

$$\frac{G(G_a - G_b)}{C_1C_2} = p_2 - q_2 \tag{14}$$

$$\frac{G_a - G_b}{LC_1C_2} = -p_3 + q_3 \tag{15}$$

or,

$$\frac{1}{C_1} = \frac{-p_1 + q_1}{G_a - G_b} \tag{16}$$

$$\frac{1}{C_2} = \frac{p_2 - q_2}{G(q_1 - p_1)} \tag{17}$$

$$\frac{1}{L} = \frac{G(q_3 - p_3)}{p_2 - q_2}. \tag{18}$$

Substituting (16), (17), and (18) into (7), (8), and (9), and after some algebraic manipulations, we obtain a set of linear algebraic equations in G, G_a, and G_b:

$$\begin{bmatrix} 0 & (p_2 - q_2) + q_1(q_1 - p_1) & q_2 - p_2 - p_1(q_1 - p_1) \\ (p_2 - q_2)(q_1 - p_1) & q_3 - p_3 - q_2(q_1 - p_1) & p_2(q_1 - p_1) - (q_3 - p_3) \\ 0 & q_3 & -p_3 \end{bmatrix} \begin{bmatrix} G \\ G_a \\ G_b \end{bmatrix} = \begin{bmatrix} 0 \\ 0 \\ 0 \end{bmatrix}. \tag{19}$$

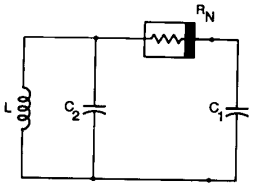

Fig. 2. The torus circuit.

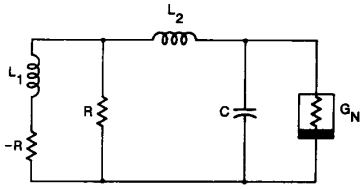

Fig. 3. The double hook circuit.

This set of homogeneous algebraic equations has nonzero solutions only if the determinant of the matrix is equal to zero, i.e.,

$$\det\begin{bmatrix}(p_2-q_2)+q_1(q_1-p_1) & (q_2-p_2)-p_1(q_1-p_1)\\ q_3 & -p_3\end{bmatrix}=0 \quad (20)$$

or

$$(p_2-q_2)(p_3-q_3)=(p_1-q_1)(p_3q_1-q_3p_1). \quad (21)$$

This is the main eigenvalue constraint on Chua's circuit. Only those eigenvalues subject to this constraint can be realized by Chua's circuit. In addition, the following obvious constraints must also be satisfied:

$$p_1\neq q_1; \qquad p_2\neq q_2; \qquad p_3\neq q_3. \quad (22)$$

Otherwise, C_1, C_2, or L will tend to infinity in view of (16)–(18).

Let us consider a numerical example using the following element parameters from Chua's circuit in [7]:

$$C_1=1/9, \quad C_2=1, \quad G=0.7, \quad G_a=-0.8$$
$$G_b=-0.5, \quad L=1/7. \quad (23)$$

Using (7)–(12), we obtain

$$p_1=0.2, \quad p_2=1.96, \quad p_3=6.3$$
$$q_1=-2.5, \quad q_2=3.85, \quad q_3=-12.6. \quad (24)$$

It is easy to verify that (24) does satisfy (21).

Consider next the piecewise-linear circuit in Fig. 2. Since it is related to the torus attractors [9], we will refer to it as the "torus circuit." By analysis similar to the above, we can show that the sets of eigenvalues of this circuit are subject to the following two constraints:

$$p_2-q_2=0 \quad (25a)$$
$$p_1q_3-p_3q_1=0. \quad (25b)$$

Comparing with (21), (25) has one more constraint on the values of p's and q's. It is understandable since the number of circuit elements in the torus circuit is smaller than that in Chua's circuit by one. Also, it is easy to see that (25) is a special case of (21). However, (25a) violates (22). Therefore, all eigenvalue sets produced by the torus circuit can *not* be produced by Chua's circuit, no matter how one adjusts the circuit parameters in this circuit.[1]

[1]This does not mean that Chua's circuit cannot display torus attractors. As a matter of fact, we have obtained torus attractors from Chua's circuit, which are associated with eigenvalues different from those in [9].

Consider next the piecewise-linear circuit in Fig. 3. We will refer to it as the "double hook circuit" [10]. By a similar analysis we can show that this circuit is also subject to the eigenvalue constraints (21) and (22), as in Chua's circuit. Hence from the point of view of computer simulation they are equivalent. However, the corresponding element parameters in these two circuits are different for a particular set of eigenvalues. From the point of view of experimental observation, one of these two circuits therefore would be a better choice if it requires fewer negative dynamic elements in a particular case.

III. The Canonical Piecewise-Linear Circuit

In this section, we will present a *universal* piecewise-linear circuit for realizing *any eigenvalue pattern* associated with any vector field in $\boldsymbol{L}$.

First we have to decide the minimum number of elements such a circuit needs. Since our objective is a three-dimensional three-region symmetric piecewise-linear continuous vector field, the circuit under consideration is allowed to have only one nonlinear resistor whose $v-i$ characteristic is three-segment piecewise-linear and symmetric with respect to the origin. The circuit must have three dynamic elements (capacitors and/or inductors) since the system is of third order. The rest are all linear resistors. Let us investigate next how many linear resistors are needed in general.

A linear autonomous RC circuit has two circuit elements and has only one natural frequency $\mu=1/RC$. If we increase C to αC and decrease R to R/α, the natural frequency of the circuit will remain unchanged. Therefore, to produce a natural frequency μ, we can assign an arbitrary value to C or R (e.g., let $C=1$) and find the value for the other parameter.

The situation is similar for Chua's circuit. In (7)–(12) there are six unknown parameters: C_1, C_2, G, G_a, G_b, and L. However, if we regard C_1, C_2, G, G_a, G_b, and $1/L$ as the unknown variables, the left-hand sides of (7)–(12) are homogeneous functions of the zeroth order. For any particular set of p's and q's, if $(C_{10}, C_{20}, G_0, G_{a0}, G_{b0}, L_0)$ is a solution of (7)–(12), then $(\alpha C_{10}, \alpha C_{20}, \alpha G_0, \alpha G_{a0}, \alpha G_{b0}, L_0/\alpha)$ (α is an arbitrary real number) will also be a solution. In other words, if (7)–(12) have solutions, we can assign an arbitrary value to any one of the six parameters (e.g., let $C_1=1$) and calculate the remaining five parameters. This means that out of the six circuit parameters, the "degree of freedom" is only five. From the point of view of circuit theory, we can refer to this observation as "impedance scaling."

The above analysis reveals why Chua's circuit cannot produce an arbitrary set of eigenvalues. There are not enough circuit parameters! Since we have six eigenvalues in our problem, we need at least seven parameters. Therefore, besides three dynamic elements and one nonlinear resistor (with the two slopes in different regions counted as two circuit parameters), we need at least two linear resistors to build a canonical circuit.

Of course, not every circuit containing that many elements will qualify as a canonical circuit. Our canonical circuit is shown in Fig. 4(a).

The state equations of this circuit are

$$\boxed{\begin{aligned}\frac{dv_1}{dt} &= \frac{1}{C_1}[-f(v_1)+i_3]\\ \frac{dv_2}{dt} &= \frac{1}{C_2}(-Gv_2+i_3)\\ \frac{di_3}{dt} &= \frac{-1}{L}(v_1+v_2+Ri_3)\end{aligned}} \tag{26}$$

where

$$f(v) = G_b v + \frac{1}{2}(G_a - G_b)(|v+1| - |v-1|) \tag{27}$$

is the $v-i$ characteristic of the nonlinear resistor shown in Fig. 4(b).

In the D_0 region (i.e., $|v_1| \leqslant 1$), the state equation (26) becomes linear:

$$\begin{bmatrix} \frac{dv_1}{dt} \\ \frac{dv_2}{dt} \\ \frac{di_3}{dt} \end{bmatrix} = \begin{bmatrix} \frac{-G_a}{C_1} & 0 & \frac{1}{C_1} \\ 0 & \frac{-G}{C_2} & \frac{1}{C_2} \\ \frac{-1}{L} & \frac{-1}{L} & \frac{-R}{L} \end{bmatrix} \begin{bmatrix} v_1 \\ v_2 \\ i_3 \end{bmatrix} = \boldsymbol{M}_0 \begin{bmatrix} v_1 \\ v_2 \\ i_3 \end{bmatrix} \tag{28}$$

where $\boldsymbol{M}_0$ is a constant matrix. The characteristic equation of $\boldsymbol{M}_0$ is

$$\begin{aligned}|s1 - \boldsymbol{M}_0| = s^3 &+ s^2\left(\frac{G_a}{C_1}+\frac{G}{C_2}+\frac{R}{L}\right)\\ &+ s\left(\frac{GG_a}{C_1C_2}+\frac{G_aR}{LC_1}+\frac{GR}{LC_2}+\frac{1}{LC_1}+\frac{1}{LC_2}\right)\\ &+ \frac{G+G_a+GG_aR}{LC_1C_2} = 0.\end{aligned} \tag{29}$$

Just as in Section II, we obtain

$$\frac{G_a}{C_1}+\frac{G}{C_2}+\frac{R}{L} = -p_1 \tag{30}$$

$$\frac{GG_a}{C_1C_2}+\frac{G_aR}{LC_1}+\frac{GR}{LC_2}+\frac{1}{LC_1}+\frac{1}{LC_2} = p_2 \tag{31}$$

$$\frac{G+G_a+GG_aR}{LC_1C_2} = -p_3. \tag{32}$$

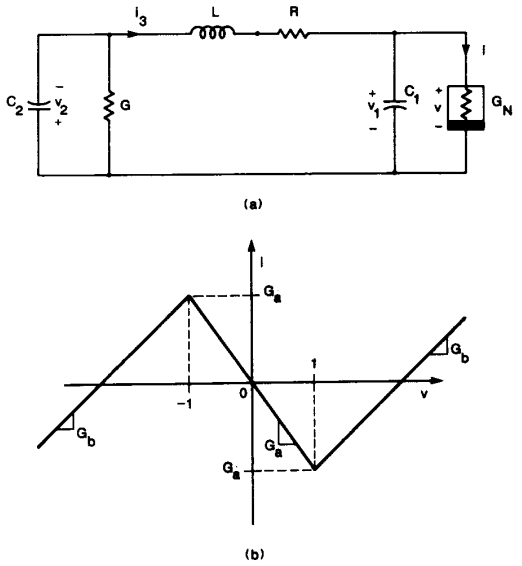

Fig. 4. (a) The canonical piecewise-linear circuit. (b) The $v-i$ characteristic of the nonlinear resistor G_N.

Similarly, from the equation in the $D_{\pm 1}$ regions (i.e., $|v_1| > 1$), we obtain

$$\frac{G_b}{C_1}+\frac{G}{C_2}+\frac{R}{L} = -q_1 \tag{33}$$

$$\frac{GG_b}{C_1C_2}+\frac{G_bR}{LC_1}+\frac{GR}{LC_2}+\frac{1}{LC_1}+\frac{1}{LC_2} = q_2 \tag{34}$$

$$\frac{G+G_b+GG_bR}{LC_1C_2} = -q_3. \tag{35}$$

Subtracting (33), (34), and (35) from (30), (31), and (32), respectively, we obtain

$$\frac{G_a-G_b}{C_1} = -p_1+q_1 \tag{36}$$

$$\frac{G_a-G_b}{C_1}\left(\frac{G}{C_2}+\frac{R}{L}\right) = p_2-q_2 \tag{37}$$

$$\frac{(G_a-G_b)(GR+1)}{LC_1C_2} = -p_3+q_3. \tag{38}$$

Substituting (36) into (37) and (38), we obtain

$$\frac{G}{C_2}+\frac{R}{L} = \frac{-p_2+q_2}{p_1-q_1} \tag{39}$$

and

$$\frac{(GR+1)}{LC_2} = \frac{p_3-q_3}{p_1-q_1}. \tag{40}$$

Substituting (39) into (30) and (33), we obtain

$$\frac{G_a}{C_1} = -p_1+\frac{p_2-q_2}{p_1-q_1} \tag{41}$$

and

$$\frac{G_b}{C_1} = -q_1 + \frac{p_2 - q_2}{p_1 - q_1}. \tag{42}$$

As mentioned before, among the seven parameters we can assign an arbitrary value to any one of them. Let us take

$$C_1 = 1. \tag{43}$$

Then we obtain the values of parameters G_a and G_b from (41) and (42):

$$G_a = -p_1 + \frac{p_2 - q_2}{p_1 - q_1} \tag{44}$$

$$G_b = -q_1 + \frac{p_2 - q_2}{p_1 - q_1}. \tag{45}$$

Substituting (39), (40), (41), and (43) into (31), we obtain the following value of L:

$$L = \frac{1}{p_2 + \left(\frac{p_2 - q_2}{p_1 - q_1} - p_1\right)\left(\frac{p_2 - q_2}{p_1 - q_1}\right) - \frac{p_3 - q_3}{p_1 - q_1}}. \tag{46}$$

Now from (32) we have

$$\frac{G}{C_2} = -L\left[p_3 + \frac{G_a(p_3 - q_3)}{C_1(p_1 - q_1)}\right] = k \tag{47}$$

where the constant k is introduced for simplicity. Substituting (47) into (39), we obtain the value of R:

$$R = -L\left(\frac{p_2 - q_2}{p_1 - q_1} + k\right). \tag{48}$$

From (40) we have

$$\frac{1}{LC_2} = \frac{p_3 - q_3}{p_1 - q_1} - \frac{GR}{LC_2} = \frac{p_3 - q_3}{p_1 - q_1} + k\left(k + \frac{p_2 - q_2}{p_1 - q_1}\right). \tag{49}$$

Hence, the value of C_2 is given by

$$C_2 = \frac{1}{L\left[\frac{p_3 - q_3}{p_1 - q_1} + k\left(k + \frac{p_2 - q_2}{p_1 - q_1}\right)\right]}. \tag{50}$$

Finally, from (47) we obtain the value of G:

$$G = kC_2. \tag{51}$$

Equations (43)–(46), (48), (50), and (51) are explicit formulas for calculating the seven parameters in our canonical circuit from *any given set* of eigenvalues. The only constraint is

$$p_1 \neq q_1. \tag{52}$$

Otherwise some of the parameters will tend to infinity. Constraint (52) is mainly academic since in the unlikely event that

$$p_1 = q_1 \tag{53}$$

for a given set of eigenvalues, we can usually eliminate this singular situation by perturbing one of the μ's or ν's without causing qualitative changes in the system's dynamics.

IV. Some Properties of the Canonical Circuit

The three-dimensional vector fields produced by our canonical circuit have the following properties.

1) The vector field is continuous everywhere and symmetric with respect to the origin.
2) The state space is partitioned into three regions D_{-1}, D_0, and D_{+1} by two parallel planes located at $v_1 = \pm 1$.
3) The vector field is linear in region D_0 and affine in regions D_{-1} and D_{+1}.

These properties are obvious from the structure of the canonical circuit. In [1] and [2], the vector fields under consideration are more restricted. They always have one equilibrium point in each region D_{-1}, D_0, and D_{+1}. Besides, the vector fields discussed in [1] all have one real eigenvalue and a pair of complex conjugate eigenvalues in each region (henceforth called *type I* eigenvalues), while those discussed in [2] all have three real eigenvalues in the D_0 region, and one real and a pair of complex conjugate eigenvalues in the $D_{\pm 1}$ regions (henceforth called *type II* eigenvalues). These two types of eigenvalue patterns are more interesting because their vector fields can exhibit chaotic attractors. However, the vector fields that can be produced by the canonical circuit have no such constraints. Their eigenvalues may be either all real, or one real plus a pair of complex conjugate values in each region. In the canonical circuit, the origin is of course an equilibrium point. However, the $D_{\pm 1}$ regions may or may not have equilibrium points. In the latter case, we say the region D_0 has two virtual equilibrium points, in addition to the equilibrium point at the origin. In [1] and [2], there are theorems stating under what condition there will be equilibrium points in regions $D_{\pm 1}$. The proofs of these theorems did not make use of any nonlinear circuit theory, and hence are quite involved and have little physical meaning. For our canonical circuit we can prove a similar theorem using a much simpler proof, which at the same time gives a much clearer physical meaning.

Theorem 1: The following three conditions are equivalent, each one giving a necessary and sufficient condition for a vector field realized by our canonical circuit to have equilibrium points in the $D_{\pm 1}$ regions.

1) The canonical circuit has three dc operating points,
2) $(G + G_a(1 + GR))(G + G_b(1 + GR)) < 0$, and (54)
3) $p_3 q_3 < 0$. (55)

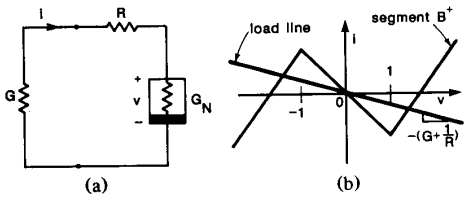

Fig. 5. (a) The dc circuit associated with the canonical piecewise-linear circuit. (b) The dc operating point of the circuit.

Proof:

1) The equilibrium points of the nonlinear system described by (26) are obtained by solving

$$\begin{aligned} f(v_1) - i_3 &= 0 \\ Gv_2 - i_3 &= 0 \\ v_1 + v_2 + Ri_3 &= 0. \end{aligned} \tag{56}$$

Equations (56) are exactly the KCL and KVL equations of the resistive circuit shown in Fig. 5(a), which is obtained from the canonical circuit with the capacitors open-circuited and the inductor short-circuited. It is obvious from the state equations (28) that the canonical circuit has one and only one equilibrium point at the origin in the D_0 region (whenever $|\boldsymbol{M}_0| \neq 0$). Hence, if the circuit has three dc operating points, two of them must be located in the $D_{\pm 1}$ regions. The converse is true, too. Fig. 5(b) gives the physical interpretation: whenever the loadline has three intersection points with the three-segment piecewise-linear characteristic, two of them must necessarily be located in the $D_{\pm 1}$ regions.

2) Segment B^+ in Fig. 5(b) is described by the equation

$$i = (G_a - G_b) + G_b v. \tag{57}$$

The loadline is described by

$$i = \frac{-v}{R + \frac{1}{G}}. \tag{58}$$

The abscissa of the intersection point of (57) and (58) is given by

$$v_0 = \frac{(G_b - G_a)(1+GR)}{G + G_b(1+GR)}. \tag{59}$$

Observe that the region D_{+1} has an equilibrium point if and only if

$$v_0 > 1. \tag{60}$$

It is easy to show that (60) is equivalent to (54) after some simple algebraic manipulations.

3) From (32) and (35), we have

$$\frac{(G + G_a(1+GR))(G + G_b(1+GR))}{L^2C_1^2C_2^2} = p_3q_3. \tag{61}$$

This implies that (54) and (55) are equivalent. □

Remark:

1) When eigenvalues are of *type I*, the signs of p_3 and q_3 are determined by the signs of γ_0 and γ_1, respectively, where γ_0 and γ_1 denote the real eigenvalues in the D_0 and $D_{\pm 1}$ regions. Therefore, (55) is equivalent to the condition

$$\gamma_0\gamma_1 < 0. \tag{62}$$

When the eigenvalues are of *type II*, the sign of p_3 is determined by the sign of $\mu_1\mu_2\mu_3$ and the sign of q_3 is determined by the sign of γ_1. Therefore (55) is equivalent to the condition

$$\mu_1\mu_2\mu_3\gamma_1 < 0. \tag{63}$$

Conditions (62) and (63) are exactly the same conditions given in [1] and [2]. We have, therefore, unified theorem 3.1 in [1] and theorem 4.1 in [2], in addition to giving an explicit physical interpretation to the theorem.

2) It is obvious from (59) that the locations of the equilibrium points depend only on the values of G, G_a, G_b, and R, and not on the values of C_1, C_2, and L.

V. Results of Computer Simulations

In this section we present a *sample* of some computer simulation results for our canonical piecewise-linear circuit.

The eigenvalue parameter space is six-dimensional. Every point in this parameter space corresponds to one or more attractors. To search and classify all possible attractors in such a huge space is a difficult project. Our simulation is by no means comprehensive. However, the simulation results presented here include not only all attractors discovered in $\boldsymbol{L}$ and reported so far in the literature, but also some newly discovered ones.

Table I shows the simulation results when the inner region contains a pair of complex conjugate eigenvalues. Table II shows the simulation results when the inner region contains only real eigenvalues. Table III summarizes the values of the eigenvalues and the circuit parameters for a sample of attractors listed in Tables I and II. Since all vector fields with the same normalized eigenvalues are linearly equivalent [1], [2], all examples in Table III have been normalized with $\omega_1 = 1$ for comparison purposes.

In Tables I and II, limit cycles have been observed for 12 different eigenvalue patterns. Most limit cycles observed have simple shapes and we therefore present only one figure (Fig. 6) for one of them. Whenever there are toroidal or chaotic attractors observed for a particular eigenvalue pattern, we give at least one example in Table III. For each attractor listed in Table III, we present a figure that is a two-dimensional projection of that attractor. Some attractors cannot be classified as toroidal or chaotic merely from a two-dimensional projection of the

TABLE I
SOME ATTRACTORS FOR TYPE I EIGENVALUE PATTERNS

	Eigenvalues				Type of stability			Observed attractors			
Class	γ_0	σ_0	γ_1	σ_1	Stable at origin?	Does $P_\pm$ exist?	Stable at $P_\pm$?	stable equilibrium	limit cycle	toroidal attractor	chaotic attractor
1	+	+	+	+	no	no		no	no	no	no
2	+	+	+	-	no	no		no	no	no	no
3	+	+	-	+	no	yes	no	no	*1	no	*2
4	+	+	-	-	no	yes	yes	yes	yes	no	no
5	+	-	+	+	no	no		no	no	no	no
6	+	-	+	-	no	no		no	no	no	no
7	+	-	-	+	no	yes	no	no	yes	*3	*4
8	+	-	-	-	no	yes	yes	yes	yes	no	no
9	-	+	+	+	no	yes	no	no	no	no	no
10	-	+	+	-	no	yes	no	no	yes	*5	*6
11	-	+	-	+	no	no		no	no	no	no
12	-	+	-	-	no	no		no	yes	no	no
13	-	-	+	+	yes	yes	no	yes	no	no	no
14	-	-	+	-	yes	yes	no	yes	no	no	no
15	-	-	-	+	yes	no		yes	no	no	no
16	-	-	-	-	yes	no		yes	no	no	no

*1: see Fig.6 for an example of a periodic attractor.
*2: see Fig.7,8,9 for examples of chaotic attractors.
*3: see Fig.10,11 for examples of toroidal attractors.
*4: see Fig.12,13,14 for examples of chaotic attractors.
*5: see Fig.15,16 for examples of toroidal attractors.
*6: see Fig.17 for an example of a chaotic attractor.

trajectory. In order to distinguish between toroidal attractors and chaotic attractors, one must usually plot cross sections of the attractors. Due to the limitation of space, however, we do not show cross sections in this paper. Also, we have omitted figures of some well-known attractors (e.g., the Double Scroll attractor).

In our simulations, chaotic attractors have been observed for six different eigenvalue patterns. These observations greatly enrich the knowledge of dynamical behaviors in the Chua's circuit family. Moreover, some interesting dynamical phenomena (e.g., intermittency) have been observed from this canonical piecewise-linear circuit, and we will report them elsewhere.

VI. An Alternative Realization of the Canonical Circuit

We do not claim that the canonical circuit in Fig. 4 is unique. However, so far we have not found any other circuit having the same degree of generality.

Fig. 21(a) shows an alternative piecewise-linear circuit. The state equations of this circuit are

$$\frac{dv_1}{dt} = \frac{1}{C_1}(-G_1 v_1 + i_3)$$

$$\frac{dv_2}{dt} = \frac{1}{C_2}(-Gv_2 + i_3)$$

$$\frac{di_3}{dt} = \frac{-1}{L}[v_1 + v_2 + f(i)] \tag{64}$$

where

$$f(i_3) = R_b i_3 + \frac{1}{2}(R_a - R_b)(|i_3 + 1| - |i_3 - 1|) \tag{65}$$

is the v–i characteristic of the nonlinear resistor shown in Fig. 21(b).

TABLE II
SOME ATTRACTORS FOR TYPE II EIGENVALUE PATTERNS

	Eigenvalues					Type of stability			Observed attractors			
Class	μ_1	μ_2	μ_3	γ_1	σ_1	Stable at origin?	Does $P_\pm$ exist?	Stable at $P_\pm$?	stable equil.	limit cycle	toroidal attractor	chaotic attractor
1	+	+	+	+	+	no	no		no	no	no	no
2	+	+	+	+	-	no	no		no	no	no	no
3	+	+	+	-	+	no	yes	no	no	yes	no	*7
4	+	+	+	-	-	no	yes	yes	yes	yes	no	no
5	+	+	-	+	+	no	yes	no	no	no	no	no
6	+	+	-	+	-	no	yes	no	no	yes	no	*8
7	+	+	-	-	+	no	no		no	no	no	no
8	+	+	-	-	-	no	no		no	yes	no	no
9	+	-	-	+	+	no	no		no	no	no	no
10	+	-	-	+	-	no	no		no	no	no	no
11	+	-	-	-	+	no	yes	no	no	yes	no	*9
12	+	-	-	-	-	no	yes	yes	yes	yes	no	no
13	-	-	-	+	+	yes	yes	no	yes	no	no	no
14	-	-	-	+	-	yes	yes	no	yes	no	no	no
15	-	-	-	-	+	yes	no		yes	no	no	no
16	-	-	-	-	-	yes	no		yes	no	no	no

*7: see Fig.18 for an example of a chaotic attractor.
*8: see Fig.19 for an example of a chaotic attractor.
*9: see Fig.20 for an example of a chaotic attractor.

In the D_0 region (i.e., $|i_3| \leqslant 1$), the state equations (64) become linear:

$$\begin{bmatrix} \frac{dv_1}{dt} \\ \frac{dv_2}{dt} \\ \frac{di_3}{dt} \end{bmatrix} = \begin{bmatrix} \frac{-G_1}{C_1} & 0 & \frac{1}{C_1} \\ 0 & \frac{-G_2}{C_2} & \frac{1}{C_2} \\ \frac{-1}{L} & \frac{-1}{L} & \frac{-R_a}{L} \end{bmatrix} \begin{bmatrix} v_1 \\ v_2 \\ i_3 \end{bmatrix} = \boldsymbol{M}_0 \begin{bmatrix} v_1 \\ v_2 \\ i_3 \end{bmatrix} \tag{66}$$

where $\boldsymbol{M}_0$ is a constant matrix. The characteristic equation of $\boldsymbol{M}_0$ is

$$|s1 - \boldsymbol{M}_0| = s^3 + s^2\left(\frac{G_1}{C_1} + \frac{G_2}{C_2} + \frac{R_a}{L}\right) + s\left(\frac{G_1G_2}{C_1C_2} + \frac{G_1R_a}{LC_1} + \frac{G_2R_a}{LC_2} + \frac{1}{LC_1} + \frac{1}{LC_2}\right) + \frac{G_1 + G_2 + G_1G_2R_a}{LC_1C_2} = 0. \tag{67}$$

It follows from (67) that

$$\frac{G_1}{C_1} + \frac{G_2}{C_2} + \frac{R}{L} = -p_1 \tag{68}$$

$$\frac{G_1G_2}{C_1C_2} + \frac{G_1R_a}{LC_1} + \frac{G_2R_a}{LC_2} + \frac{1}{LC_1} + \frac{1}{LC_2} = p_2 \tag{69}$$

$$\frac{G_1 + G_2 + G_1G_2R_a}{LC_1C_2} = -p_3. \tag{70}$$

Similarly, from the equation in the $D_{\pm 0}$ regions (i.e., $|i_3| > 1$) we obtain

$$\frac{G_1}{C_1} + \frac{G_2}{C_2} + \frac{R_b}{L} = -q_1 \tag{71}$$

$$\frac{G_1G_2}{C_1C_2} + \frac{G_1R_b}{LC_1} + \frac{G_2R_b}{LC_2} + \frac{1}{LC_1} + \frac{1}{LC_2} = q_2 \tag{72}$$

$$\frac{G_1 + G_2 + G_1G_2R_b}{LC_1C_2} = -q_3. \tag{73}$$

Subtracting (71), (72), and (73) from (68), (69), and (70),

TABLE III
PARAMETERS OF THE CANONICAL CIRCUIT ASSOCIATED WITH DIFFERENT ATTRACTORS IN FIGS. 6–20

	Eigenvalues*					Circuit parameters*					
Fig.	μ_1	μ_2	μ_3	γ_1	σ_1	C_2	G	G_a	G_b	L	R
6	0.30	0.20	±j20.0	-20.0	0.20	1513	-492.4	19.35	39.65	.00128	-0.0252
7	0.20	0.30	±j10.0	-3.0	0.30	11183	-2565	30.73	33.93	.00094	-.02947
8	0.30	.0577	±j2.78	-1.33	0.29	170.0	-86.0	5.98	7.146	.0234	-.1376
9	0.44	.0577	±j2.78	-1.33	0.29	105.0	-70.3	5.17	6.47	.0297	-0.15
10	.1474	-.0487	±j1.0	-.104	.0343	-0.66	0.071	-0.12	-.036	-.050	-.090
11	.272	-.0635	±j.746	-.076	.0019	22.1	11.1	-2.33	-2.11	.220	.368
12	.272	-.136	±j.409	-.409	.0454	48.4	31.6	-2.68	-2.36	.171	.346
13	1.474	-.0487	±j1.0	-1.04	.0343	-.154	.0285	-1.41	.941	-5.82	-1.25
14	.618	-.370	±j3.50	-2.30	.195	99.6	-89.4	6.72	8.50	.020	-.113
*1	.728	-.319	±j.892	-1.29	.061	-.632	-.0033	-.419	.839	-1.02	-.330
*2	.728	-.319	±j.892	-1.29	.042	-0.60	0.01	-.445	.851	-1.10	-.409
15	-.050	.080	±j1.0	.035	-.056	-3.19	.0042	-.114	.0726	.687	.0039
16	-1.62	.084	±j1.15	.922	-.412	-0.70	-.0015	1.034	-.515	-.685	-.285
17	-.450	.0235	±j.346	.277	-.124	41.1	-18.5	2.36	1.93	.252	-.381
18	6.80	4.30	2.50	-9.0	0.01	12.30	-15.64	-11.1	11.47	.0389	-.0473
19	1.032	.1354	-.4425	.020	-.20	-95.68	3.733	-2.0	-.895	.4448	.5845
20	.919	-.541	-3.64	-.353	.156	-15.6	-6.42	4.13	.906	.421	-.537
*3	1.15	-2.98	-5.70	-.89	.150	-1.35	.0014	6.63	-.310	.251	.226

*: The parameters ω_1 and C_1 for all attractors are assumed to be equal to 1.

*1: A Double Scroll attractor. The same as Fig.2 of [7].

*2: A Rössler's spiral-type attractor. The same as Fig.8 of [8].

*3: A Double Hook attractor. The same as Fig.3 of [10].

respectively, we obtain

$$\frac{R_a - R_b}{L} = -p_1 + q_1 \tag{74}$$

$$\frac{R_a - R_b}{L}\left(\frac{G_1}{C_1} + \frac{G_2}{C_2}\right) = p_2 - q_2 \tag{75}$$

$$\frac{G_1 G_2 (R_a - R_b)}{LC_1C_2} = -p_3 + q_3. \tag{76}$$

Substituting (74) into (75) and (76), we obtain

$$\frac{G_1}{C_1} + \frac{G_2}{C_2} = \frac{-p_2 + q_2}{p_1 - q_1} \tag{77}$$

and

$$\frac{G_1 G_2}{C_1 C_2} = \frac{p_3 - q_3}{p_1 - q_1}. \tag{78}$$

Since one parameter can be assigned an arbitrary value, let us take

$$L = 1. \tag{79}$$

Substituting (77) and (78) into (68) and (71), we obtain the following values of R_a and R_b:

$$R_a = -p_1 + \frac{p_2 - q_2}{p_1 - q_1} \tag{80}$$

$$R_b = -q_1 + \frac{p_2 - q_2}{p_1 - q_1}. \tag{81}$$

On the other hand, (77) and (78) imply that G_1/C_1 and G_2/C_2 are the two roots of the following quadratic equation:

$$x^2 + x\left(\frac{p_2 - q_2}{p_1 - q_1}\right) + \frac{p_3 - q_3}{p_1 - q_1} = 0. \tag{82}$$

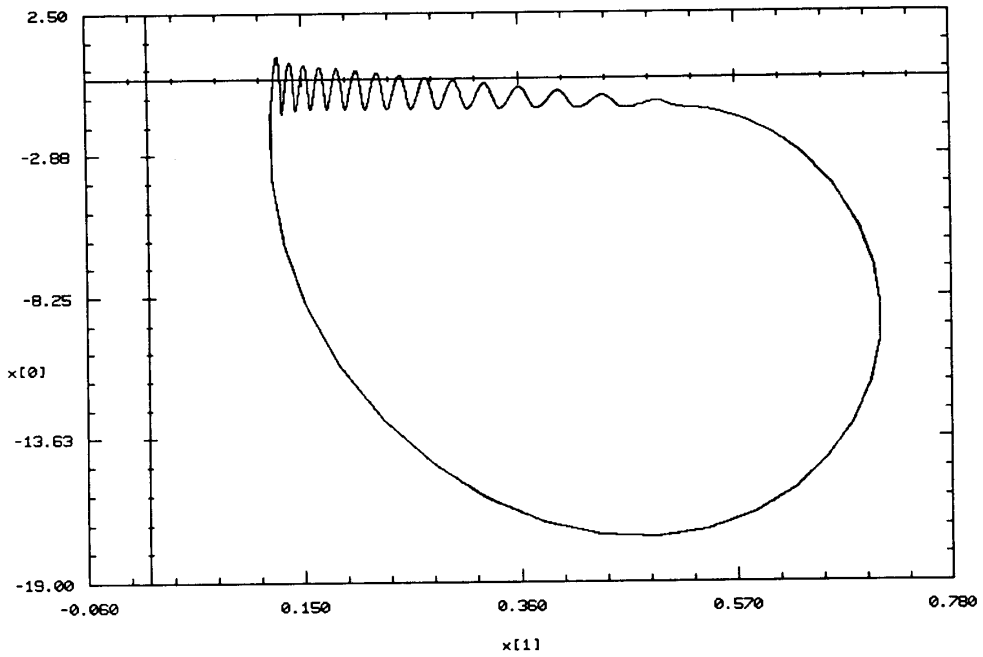

Fig. 6. An example of a limit cycle associated with a type I class 3 eigenvalue pattern. (Projection onto the (v_2, v_1)-plane.)

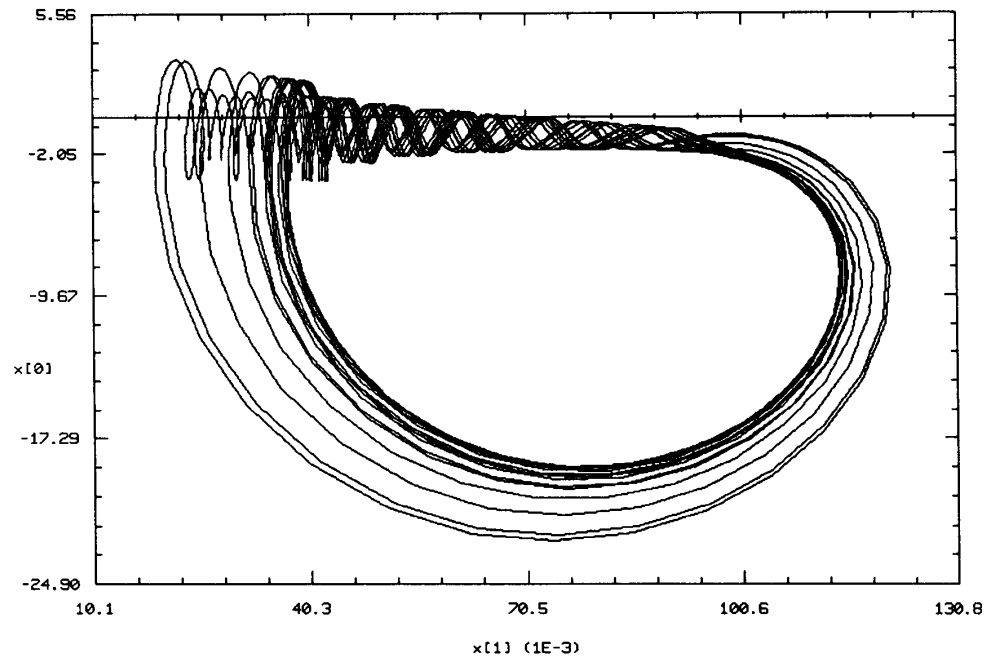

Fig. 7. An example of a chaotic attractor associated with a type I class 3 eigenvalue pattern. (Projection onto the (v_2, v_1)-plane.)

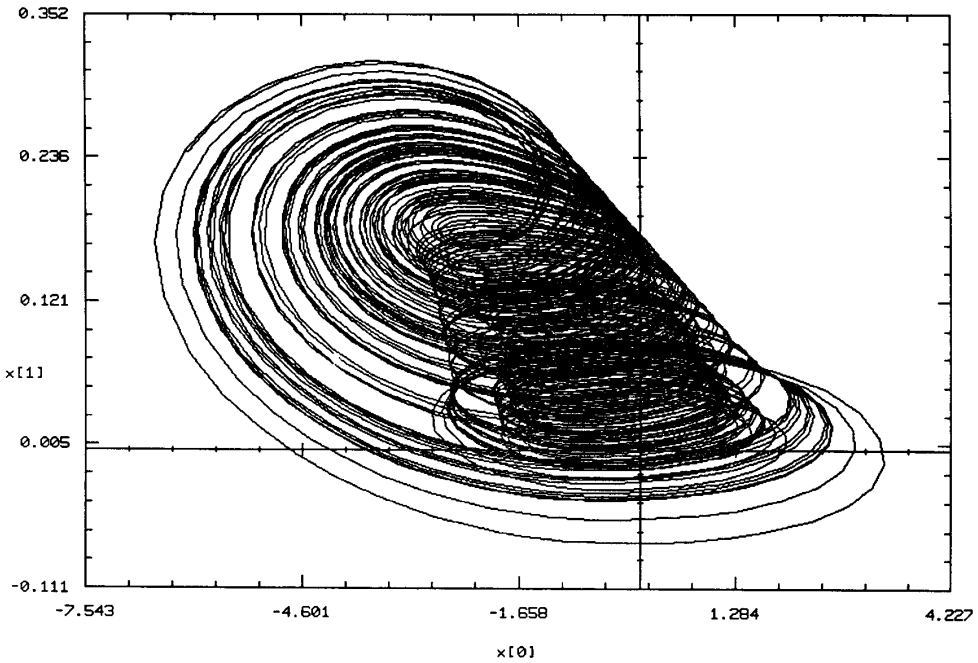

Fig. 8. An example of a chaotic attractor associated with a type I class 3 eigenvalue pattern. (Projection onto the (v_1, v_2)-plane.)

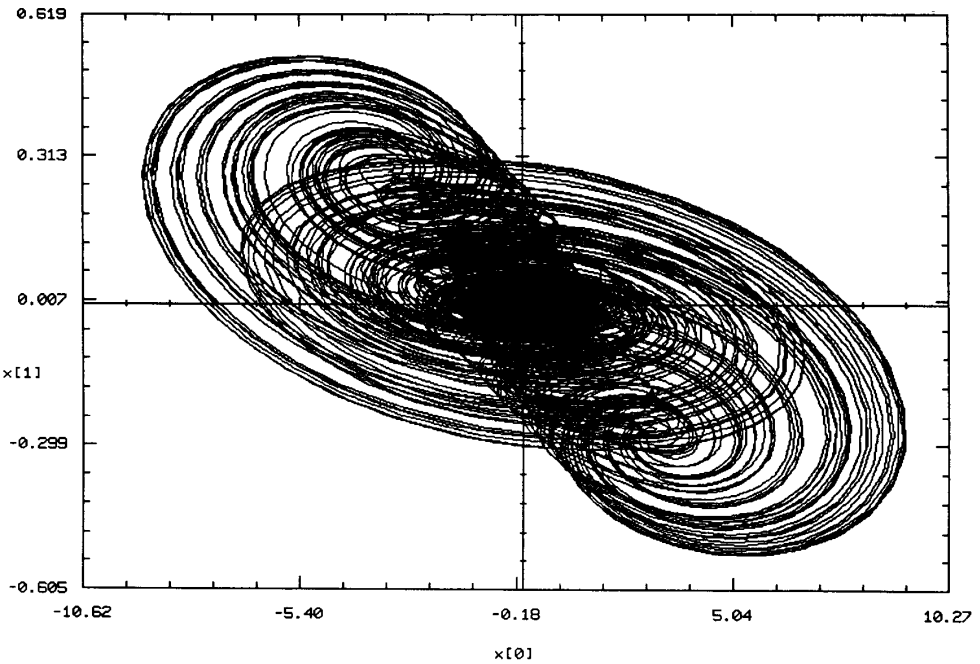

Fig. 9. An example of a chaotic attractor associated with a type I class 3 eigenvalue pattern. (Projection onto the (v_1, v_2)-plane.)

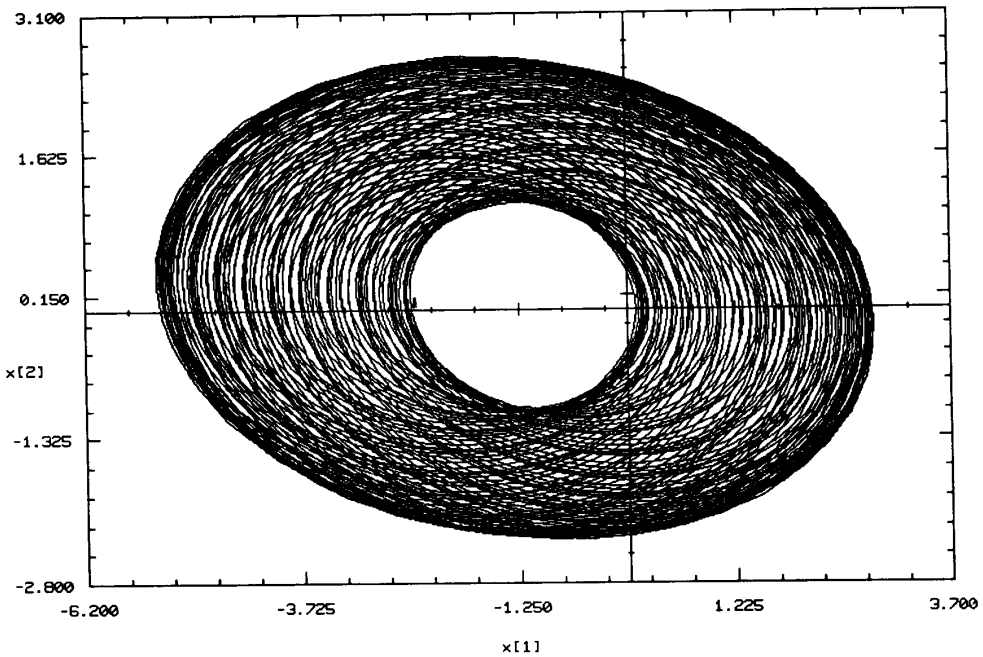

Fig. 10. An example of a toroidal attractor associated with a type I class 7 eigenvalue pattern. (Projection onto the (v_2, i_3)-plane.)

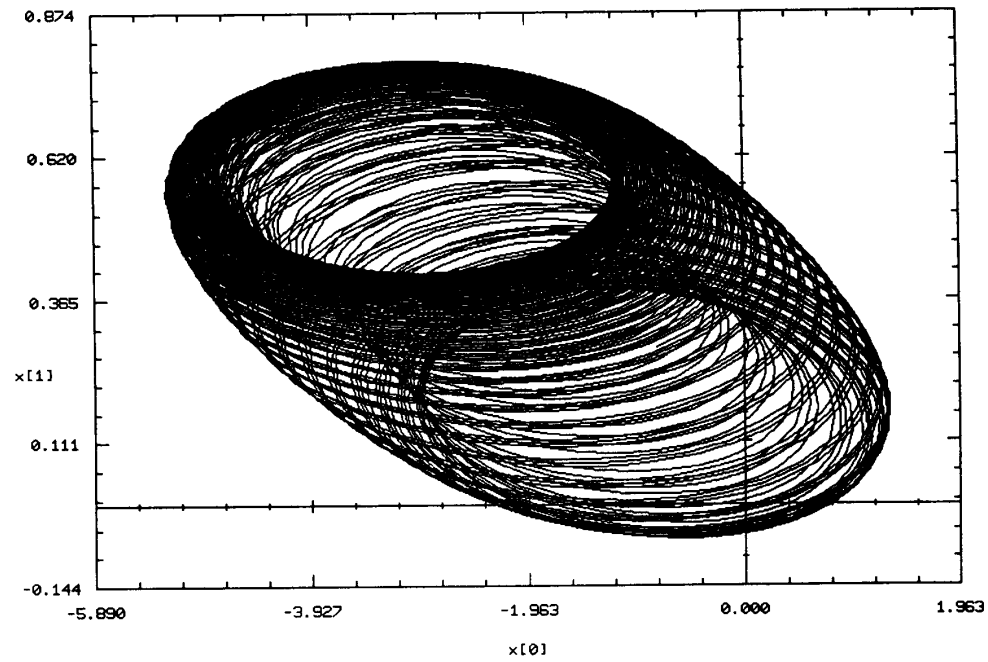

Fig. 11. An example of a toroidal attractor associated with a type I class 7 eigenvalue pattern. (Projection onto the (v_1, v_2)-plane.)

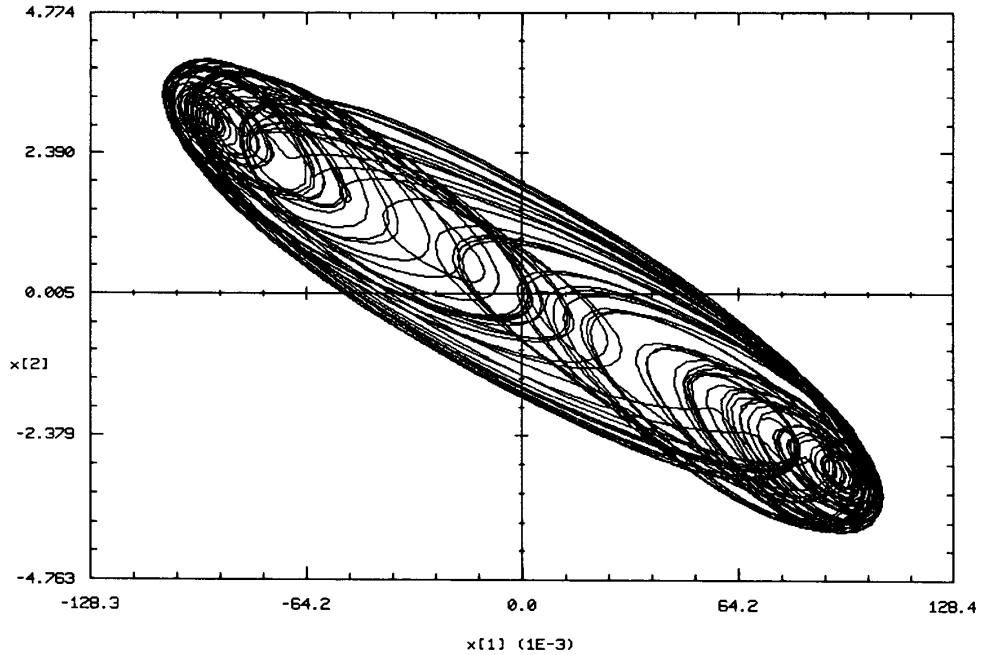

Fig. 12. An example of a chaotic attractor associated with a type I class 7 eigenvalue pattern. (Projection onto the (v_2, i_3)-plane.)

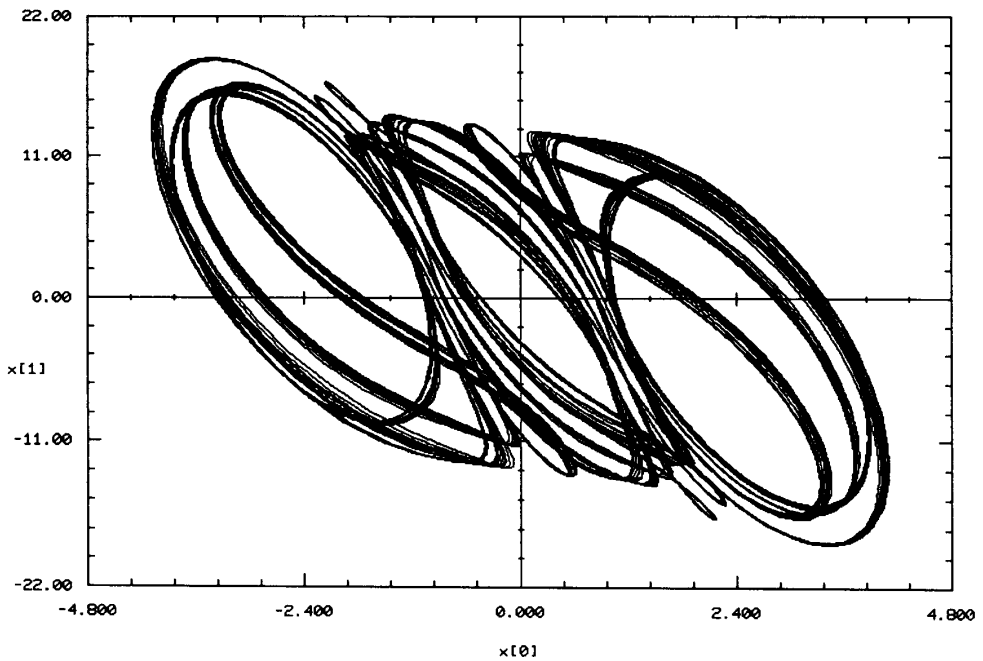

Fig. 13. An example of a chaotic attractor associated with a type I class 7 eigenvalue pattern. (Projection onto the (v_1, v_2)-plane.)

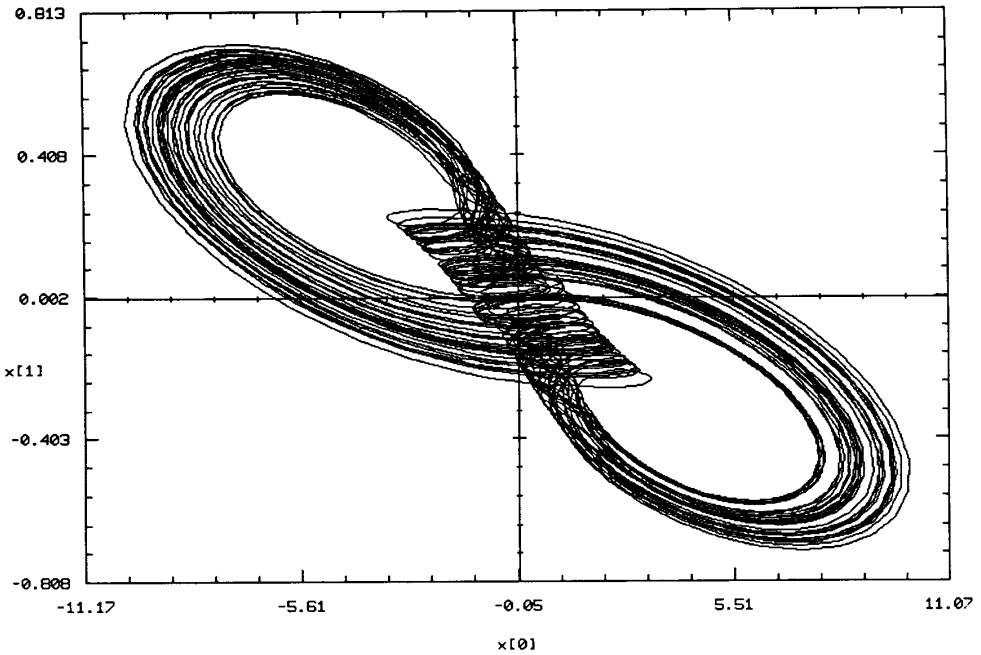

Fig. 14. An example of a chaotic attractor associated with a type I class 7 eigenvalue pattern. (Projection onto the (v_1, v_2)-plane.)

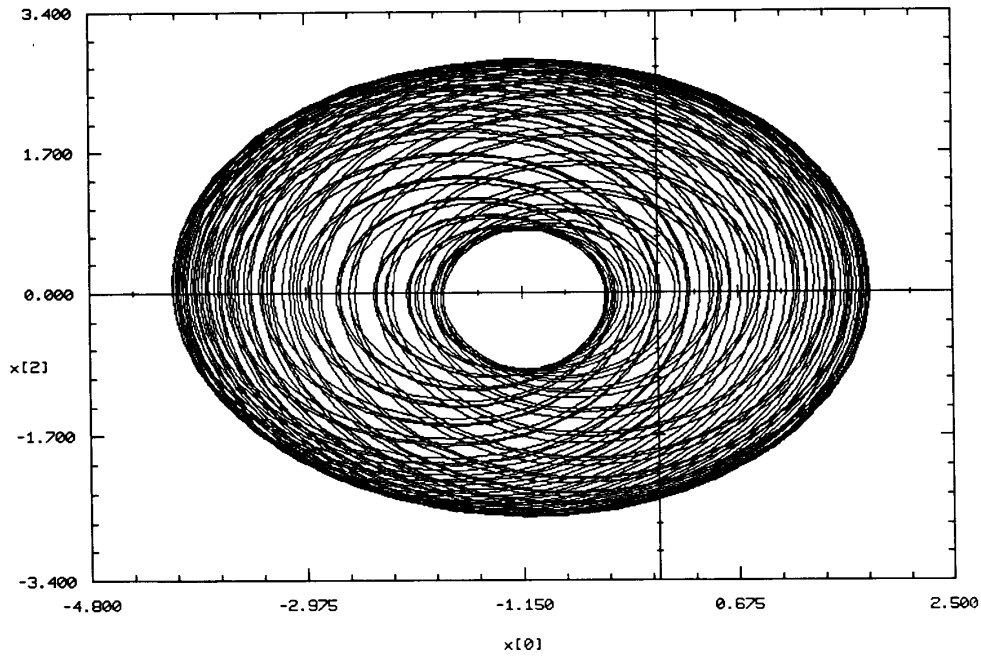

Fig. 15. An example of a toroidal attractor associated with a type I class 10 eigenvalue pattern. (Projection onto the (v_1, i_3)-plane.)

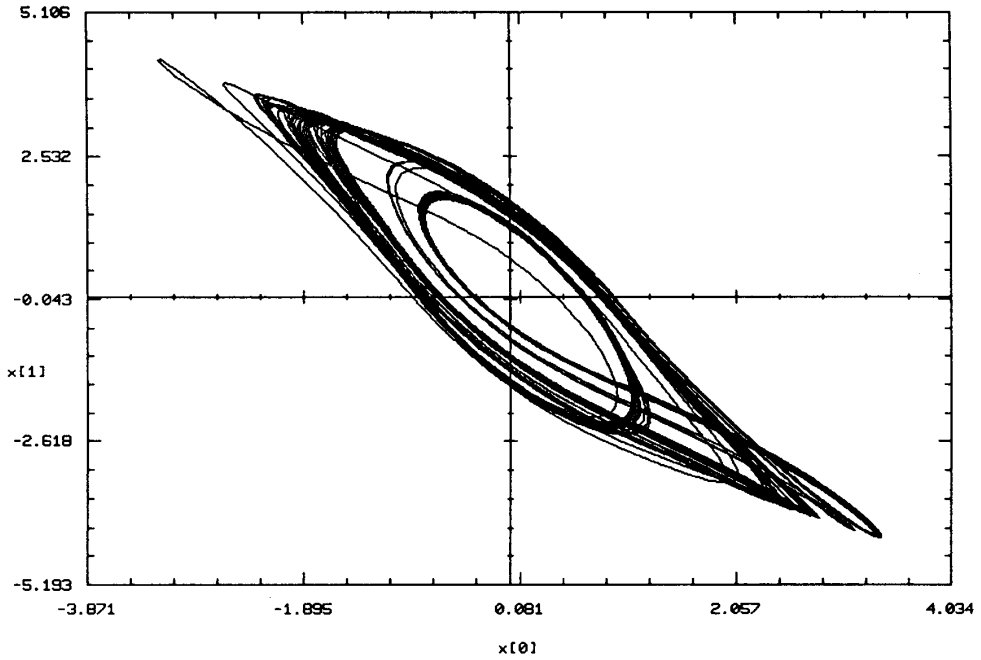

Fig. 16. An example of a toroidal attractor associated with a type I class 10 eigenvalue pattern. (Projection onto the (v_1, v_2)-plane.)

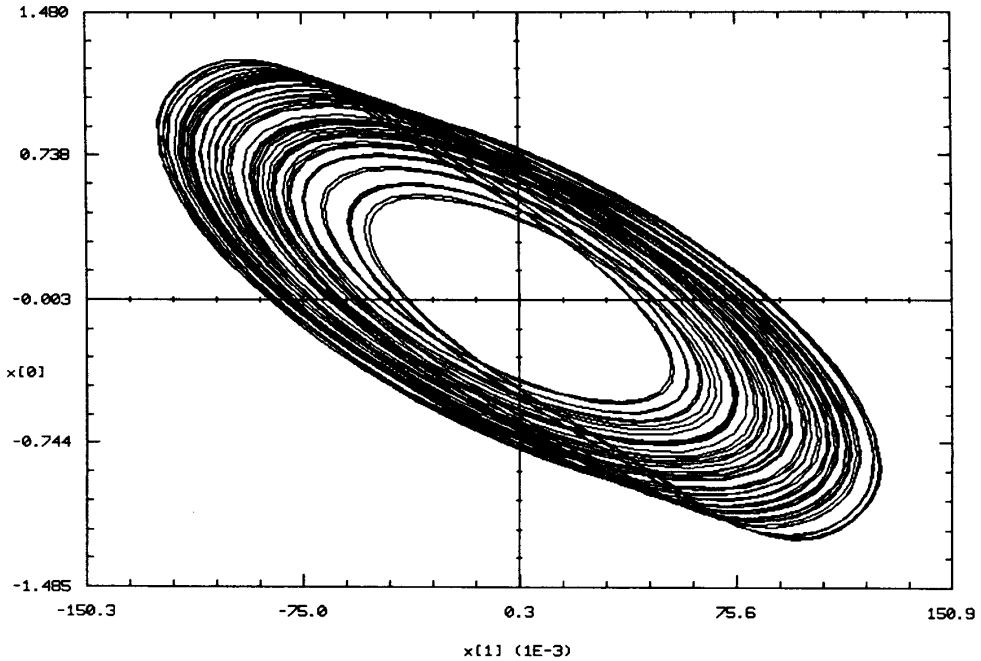

Fig. 17. An example of a chaotic attractor associated with a type I class 10 eigenvalue pattern. (Projection onto the (v_2, v_1)-plane.)

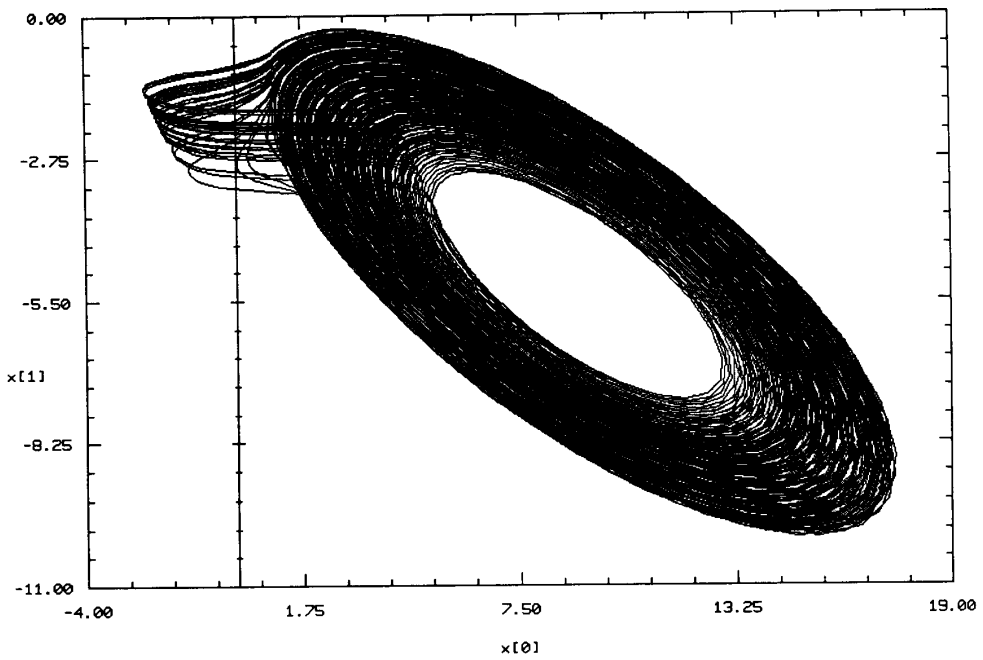

Fig. 18. An example of a chaotic attractor associated with a type II class 3 eigenvalue pattern. (Projection onto the (v_1, v_2)-plane.)

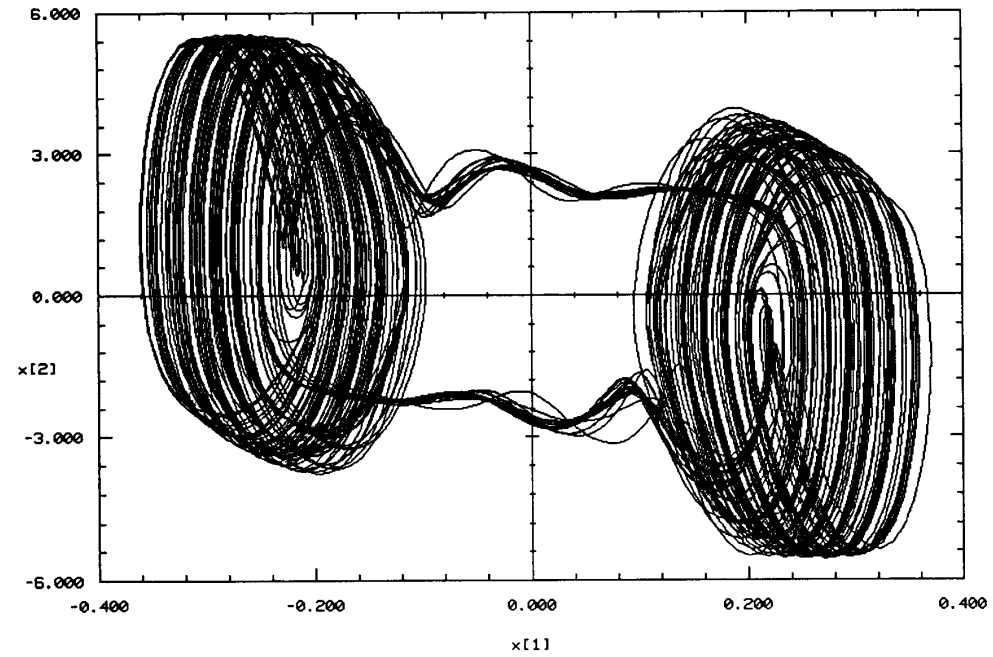

Fig. 19. An example of a chaotic attractor associated with a type II class 6 eigenvalue pattern. (Projection onto the (v_2, i_3)-plane.)

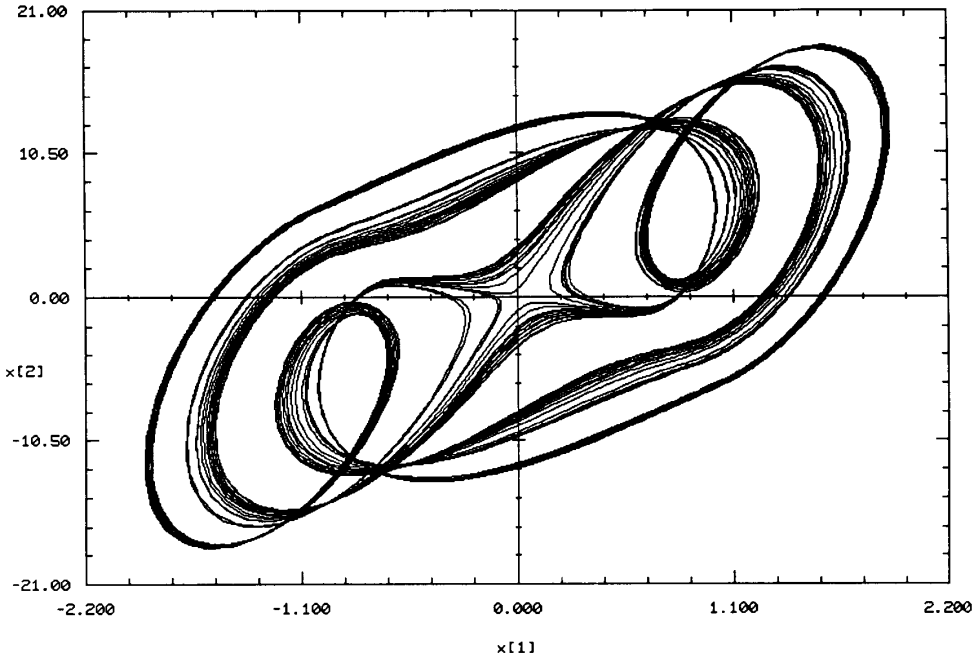

Fig. 20. An example of a chaotic attractor associated with a type II class 11 eigenvalue pattern. (Projection onto the (v_2, i_3)-plane.)

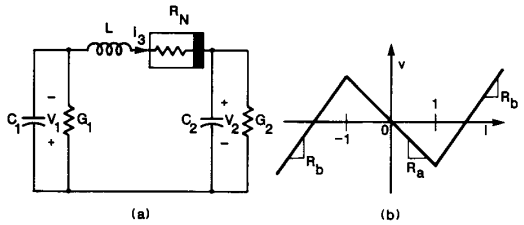

Fig. 21. (a) An alternative but less general piecewise-linear circuit. (b) The $v-i$ characteristic of the nonlinear resistor R_N.

Solving for the values of G_1/C_1 and G_2/C_2, we obtain

$$\frac{G_1}{C_1} = \frac{-p_2+q_2+\sqrt{(p_2-q_2)^2-(p_1-q_1)(p_3-q_3)}}{2(p_1-q_1)} \triangleq k_1 \tag{83}$$

$$\frac{G_2}{C_2} = \frac{-p_2+q_2-\sqrt{(p_2-q_2)^2-(p_1-q_1)(p_3-q_3)}}{2(p_1-q_1)} \triangleq k_2. \tag{84}$$

Substituting (78), (79), (80), (83), and (84) into (69) and (70), we obtain

$$\frac{1}{C_1}+\frac{1}{C_2} = p_2 - \frac{p_3-q_3}{p_1-q_1} + \frac{p_2-q_2}{p_1-q_1}\left(\frac{p_2-q_2}{p_1-q_1}-p_1\right) \tag{85}$$

$$\frac{k_1}{C_1}+\frac{k_2}{C_2} = -p_3 - \frac{p_3-q_3}{p_1-q_1}\left(\frac{p_2-q_2}{p_1-q_1}-p_1\right). \tag{86}$$

Equations (85) and (86) constitute a system of two linear algebraic equations in $1/C_1$ and $1/C_2$, which is easy to solve. Finally, we can calculate G_1 and G_2 from (83) and (84):

$$G_1 = k_1 C_1 \tag{87}$$

$$G_2 = k_2 C_2. \tag{88}$$

Since all circuit parameters can be explicitly calculated from the given set of eigenvalues, this circuit seems qualified as an alternative canonical circuit. However, it is subject to a somewhat stronger restriction than the canonical circuit proposed in Section III. This is because (83) and (84) have real solutions only if

$$(p_2-q_2)^2 \geq 4(p_1-q_1)(p_3-q_3). \tag{89}$$

Therefore, it is not general enough to qualify as a canonical circuit. If we are only interested in computer simulation, the canonical circuit in Fig. 4 is more than adequate and there is no need to search for alternative circuits. However, our canonical circuit may contain some *negative* dynamic elements for some sets of eigenvalues. In the laboratory, negative C and L are usually harder to realize than negative R. Consequently, if another circuit can produce the same vector field but contains fewer negative dynamic elements, then it may be preferable to use such an alternative equivalent circuit for practical realization purposes.

VII. Concluding Remarks

We have developed a canonical circuit that is general enough for simulating all possible dynamics associated with any three-dimensional three-region and symmetric

piecewise-linear continuous vector field. It contains only one three-segment piecewise-linear resistor and the least number of two-terminal linear elements. Moreover, it requires no controlled sources. All circuit parameters can be determined *uniquely* and *explicitly* from any given set of eigenvalues with no constraints. It would of course be highly desirable to derive analogous canonical circuits for higher dimensional systems.

REFERENCES

[1] L. O. Chua, M. Komuro, and T. Matsumoto, "The double scroll family," *IEEE Trans Circuits Syst.*, vol. CAS-33, pp. 1073–1118, Nov. 1986.

[2] C. P. Silva and L. O. Chua, "The overdamped double-scroll family," *Inter. J. Circuit Theory Appl.*, vol. 16, pp. 233–302, 1988.

[3] C. T. Sparrow, "Chaos in a three-dimensional single loop feedback system with a piecewise-linear feedback function," *J. Math. Anal. Appl.*, vol. 83, pp. 275–291, 1981.

[4] J. N. Schulman, "Chaos in piecewise-linear systems," *Phys. Rev.* A28, pp. 477–479, 1983.

[5] C. Kahlert and L. O. Chua, "Transfer maps and return maps for piecewise-linear three-region dynamical systems," *Int. J. Circuit Theory Appl.*, vol. 15, pp. 23–49, 1987.

[6] S. Wu, "Chua's circuit family," *Proc. IEEE*, vol. 75, pp. 1022–1032, Aug. 1987.

[7] T. Matsumoto, L. O. Chua, and M. Komuro, "The double scroll," *IEEE Trans. Circuits Syst.*, vol. CAS-32, pp. 797–818, Aug. 1985.

[8] ___, "The double scroll bifurcation," *Int. J. Circuit Theory Appl.*, vol. 14, pp. 117–146, 1986.

[9] T. Matsumoto, L. O. Chua, and M. Tokunaga, "Chaos via torus breakdown," *IEEE Trans. Circuits Syst.*, vol. CAS-34, pp. 240–253, Mar. 1987.

[10] P. Bartissol and L. O. Chua, "The double hook," *IEEE Trans. Circuits Syst.*, vol. 35, pp. 1512–1522, Dec. 1988.

✠

Leon O. Chua (S'60–M'62–SM'70–F'74), for a biography and photo, please see p. 383 of the March 1990 issue of this TRANSACTIONS.

✠

Gui-nian Lin received the diploma in electrical engineering from the Shanghai Jiaotong University, Shanghai, China in 1962 and the diploma in circuit theory from the Graduate Division of the same university in 1966.

From 1966 to 1973 he was with the Shanghai Jiao-tong University. In 1973 he joined the Department of Electrical Engineering at the Shanghai Railroad Institute, where he is currently an Associate Professor. During 1980–1982 and 1988–1990, he was with the Electronics Research Laboratory, University of California, Berkelely, as a visiting scholar. His research interest include general circuit theory and nonlinear dynamics.